JOURNAL OF MATERIALS SCIENCE 17 (1982) 2757–2769

Production of strontium-substituted lanthanum manganite perovskite powder by the amorphous citrate process

M. S. G. BAYTHOUN, F. R. SALE
Metallurgy Department, University of Manchester, Manchester, UK

The amorphous citrate process has been used to produce Mn_2O_3, Mn_3O_4, $LaMnO_3$, $SrMnO_3$ and strontium-substituted $LaMnO_3$. The citrate-nitrate gels were dehydrated at 70° C to yield solid precursor materials. The decomposition/oxidation of the precursors have been studied using thermogravimetry and evolved gas analysis. The products of decomposition have been characterized by X-ray diffraction analysis, scanning electron microscopy and, in the case of the strontium-substituted $LaMnO_3$, by analytical electron microscopy. The surface area and residual carbon content of the strontium-substituted $LaMnO_3$ have been determined as a function of the decomposition/oxidation temperature. Both the process yield and compositional homogeneity of the strontium-substituted $LaMnO_3$ have been shown to increase as the decomposition temperature increases. The residual carbon content has been shown to decrease as decomposition temperature increases. However, the surface areas of the powders decrease significantly as decomposition temperature increases. Consequently, it is evident that there is a conflict in the experimental conditions required for optimum yield, homogeneity and residual carbon content compared to those required for maximum surface area.

1. Introduction

Over recent years specialized preparative techniques such as freeze-drying [1–4] and various types of gel processes [5–7] have been used to produce oxides in a fine particulate form. These techniques have also been extended to applications in which uniform chemical homogeneity, as well as small particle size, are required in the product [8–10]. In particular the amorphous citrate process has been shown to have great potential because of the high yields of uniformly substituted complex perovskite oxides that may be obtained [10].

The electrical properties of certain lanthanum perovskites, in which part of the lanthanum content is substituted by strontium, have shown these oxides to have potential use as resistors and high-temperature electrodes in the electrical industry [11]. However, from the proposed mechanism of electrical conduction, it is evident that the homogeneity of substitution of the strontium ions within the perovskite lattice is an important factor in the use of the perovskite. The conventional methods of preparation of the perovskites usually rely upon the repeated sintering and milling of oxide mixtures or oxide/carbonate mixtures such that the required substituted perovskite is obtained as a result of solid-state diffusion processes. Using such a technique the times required to obtain acceptable homogeneity may be very extensive. Consequently, it is evident that the use of the amorphous citrate process in which the homogeneity of an aqueous solution of salts is preserved in a gel and possibly into the final solid oxide product may offer significant advantages in the production of substituted oxides of high homogeneity.

Previous work [10] has studied the production of strontium-substituted lanthanum cobaltite and lanthanum chromite and it was anticipated that a useful extension of this work would be the preparation and characterization of strontium-substituted

0022–2461/82/092757–13$04.06/0

lanthanum manganite because, as well as being of interest because of its electrical properties, much interest has been expressed in the use of the manganite as a catalyst for the oxidation of carbon monoxide in automobile exhausts [12, 13]. In these catalytic applications the homogeneity of substitution of strontium in the perovskite is again of great importance.

To investigate the applicability of the amorphous citrate process to the production of the manganite perovskite it was necessary to study the production and decomposition of amorphous citrate precursors of the oxides Mn_2O_3, $LaMnO_3$, $SrMnO_3$ and $La_{(1-x)}Sr_xMnO_3$ in order to understand the reaction mechanisms involved in the process. The intermediate products and resultant oxides were characterized and the homogeneity of the substituted perovskite was determined by analytical electron microscopy.

2. Experimental procedure

2.1. Preparation of the amorphous citrate precursors

"Analar" grade citric acid and the metal nitrates in the required proportions were each dissolved in 10 ml distilled water, although more dilute solutions using 20 ml water were also investigated for the production of the precursor of Mn_2O_3. The individual solutions for each precuror were then mixed together to produce the required gels. The compositions of the various starting solutions are given in Table I. In all cases the minimum amount of citric acid used was that necessary to bind the metals if all the NO_3^- ions were replaced. The water was evaporated from the solutions under vacuum in a revolving flask held at 60 to 80° C until a viscous liquid was obtained. This liquid was transferred to an evaporating basin and was maintained in a vacuum oven at 70 ± 5° C for up to 12 h in order to produce the required precursors.

2.2. Thermal decomposition and thermal stabilities of the precursors

The thermal stabilities of the precursors were studied in order to gain some understanding of the mechanisms of decomposition, to determine any unwanted compounds that may be produced during thermal decomposition and to determine the conditions required for the preparation of the strontium-substituted lanthanum manganite. Thermogravimetry and evolved gas analysis were used to study the decomposition of the precursors, manganese nitrate ($Mn(NO_3)_2 \cdot 4H_2O$), lanthanum nitrate ($La(NO_3)_3 \cdot 6H_2O$), strontium nitrate ($Si(NO_3)_2$) and strontium carbonate. The thermogravimetric studies were carried out using a "Stanton" automatic recording balance (sensitivity ± 0.0001 g) with a sample weight of approximately 0.1 g. The samples were heated from room temperature up to a maximum of 1300° C at a rate of 6° C min^{-1}. On the basis of the data obtained from the automatic balance, larger batches of precursor were decomposed in a platinum-wound furnace at temperatures up to 1400° C in order to produce quantities of oxides for subsequent characterization.

Evolved gas analysis was performed using a "V.G. micromass 6" mass spectrometer fitted with a residual gas analysis source. The gases were sampled from a silica reaction vessel which was positioned in a furnace than was temperature-programmed by a Stanton-Redcroft linear programmer. The mass spectrometer was fitted with a 90° sector, 6 cm radius electromagnetic analyser. The resolving slit was 0.05 mm which gave a resolution of approximately 400 at mass 40. A Faraday plate collector and amplifier were used as the ion detector. In operation approximately 0.05 g precursor was heated at a rate of 5° C min^{-1} up to approximately 1100° C as air or oxygen was bled into the silica reactor. The mass spectrometer

TABLE I Solutions used for production of precursors

Precursor of:	Initial solutions							
	$Mn(NO_3)_2 \cdot 4H_2O$		$La(NO_3)_3 \cdot 6H_2O$		$Sr(NO_3)_2$		Citric acid	
	Mass (g)	Water (ml)	Mass (g)	Water (ml)	Mass (g)	Water (ml)	Mass (g)	Water (ml)
Mn_2O_3	2.5112	10					2.1014	10
Mn_2O_3	2.5112	20					2.1014	20
$LaMnO_3$	2.5112	10	4.3302	10			4.2028	10
$La_{0.5}Sr_{0.5}MnO_3$	2.5112	10	2.1651	10	1.0581	10	4.2028	10
$SrMnO_3$	2.5112	10			2.1163	10	4.2028	10

was operated to scan continuously over the mass number range 10–46.

2.3. Characterization of precursors and products

X-ray diffraction analysis using CuKα radiation and a "Philips" powder camera was carried out for the precursors, the products obtained at various stages of decomposition and the final products of decomposition of the precursors. The particle morphologies of all samples (precursors and products) were studied using a "Cambridge 180" scanning electron microscope. Analytical electron microscopy was performed on the strontium-substituted perovskite using "EMMA-4" fitted with an energy dispersive solid-state detector. Standard copper grids were coated with a thin layer of carbon, dipped into a suspension of the particles in methanol, dried and then positioned in the microscope. Microanalysis was carried out at a magnification of x 16 000 and a beam diameter of 20×10^3 nm. Surface-area measurements of the various powder samples were carried out using the "Quantachrome-Quantasorb" BET absorption technique. Pure nitrogen gas was used for calibration of the instrument in quantities such that the calibration volume always produced a signal with a peak height within 15% of that obtained on desorption from the powder sample under study. The single point BET method was used in each case [14]. Carbon analysis of the strontium-substituted manganite was performed using a simple combustion technique in which the samples were heated at 1100° C in pure oxygen and the CO_2 produced by combustion was collected on soda asbestos.

3. Results

3.1. Decomposition of the precursors

The results of the thermogravimetric and evolved gas analysis studies of the decomposition/oxidation of the citrate-nitrate precursors are summarized in Figs 1 to 4. The percentage weight losses of the precursors that were decomposed in the platinum-wound furnace were consistent with those obtained in the thermogravimetric studies. In all cases the actual weight losses were significantly lower than those predicted on the basis of the stoichiometries of nitrate and citrate used in the original solutions for the production of the gels. The predicted and observed weight losses are presented in Table II.

The X-ray diffraction analyses of the precursors

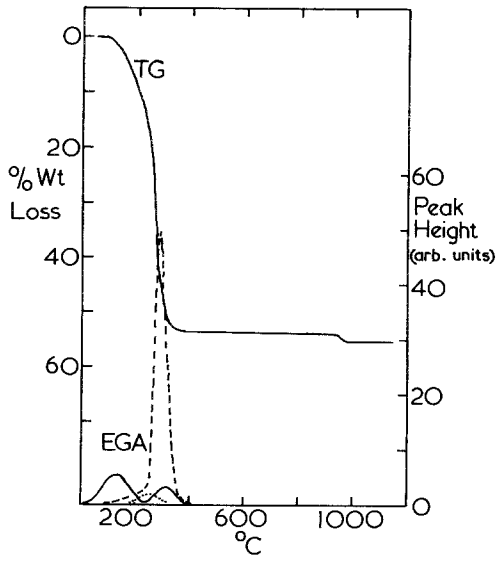

Figure 1 TG and EGA data for decomposition/oxidation of precursor of Mn_2O_3. – – – m/e 44; ------ m/e 30; ——— m/e 18.

and the products obtained at various stages of the decomposition processes are summarized in Table III where it can be seen that the precursors of Mn_2O_3 and $LaMnO_3$ were amorphous whereas both the precursors containing strontium showed some evidence of the presence of strontium nitrate which had separated from the gel during the initial stages of processing. In addition, strontium carbonate was found in the strontium-substituted lanthanum precursor at room temperature and in both samples that contained strontium after decomposition at elevated temperature. The various compounds were identified

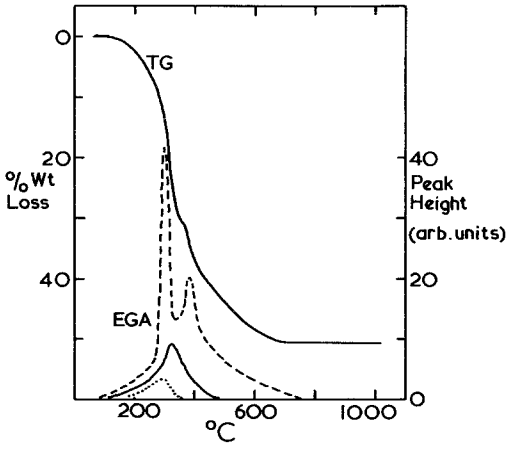

Figure 2 TG and EGA data for decomposition/oxidation of precursor of $LaMnO_3$. – – – m/e 44; ------ m/e 30; ——— m/e 18.

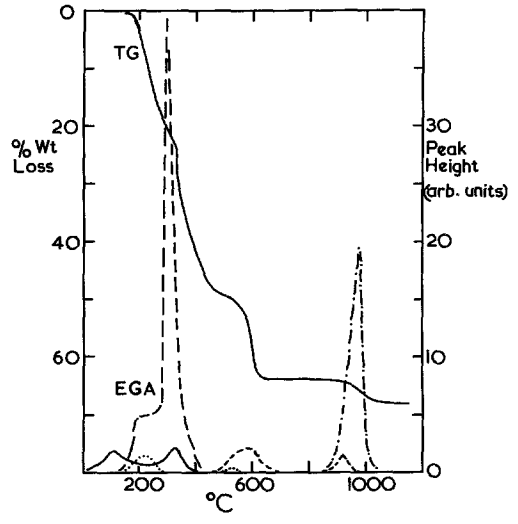

Figure 3 TG and EGA data for decomposition/oxidation of precursor of $SrMnO_3$. – – – m/e 44; ------ m/e 30; ——— m/e 18; ·—·— 28.

by comparison of the experimental data with that contained in the ASTM index for identical or similar compounds.

The carbon contents of the $La_{1-x}Sr_xMnO_3$ products obtained on decomposition of the precursor at different temperatures are presented in Table IV.

3.2. Particle characterization

Representative scanning electron micrographs of various intermediate and final products of thermal decomposition/oxidation of the precursors are

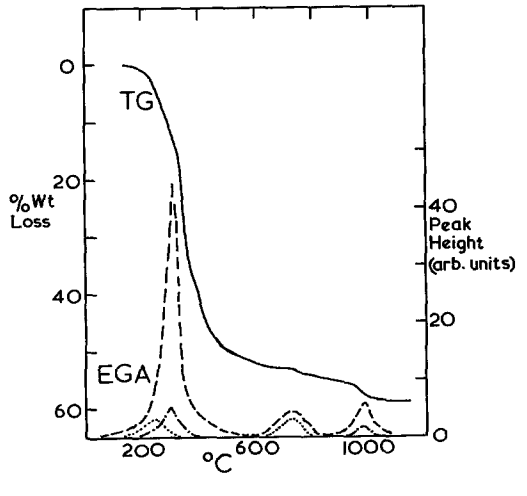

Figure 4 TG and EGA data for decomposition/oxidation of precursor of $Sr_{0.5}La_{0.5}MnO_3$. – – – m/e 44; ------ m/e 30; ·—·— 28.

TABLE II Observed and predicted weight losses for precursor decomposition/oxidation

Precursor of:	Observed % original wt (average of four)	Predicted on basis of citric acid and nitrate used (excluding water of crystallization)
Mn_2O_3	55.5 ± 0.4	78.7
$LaMnO_3$	50.6 ± 0.5	78.1
$SrMnO_3$	66.0 ± 0.5	78.4
$(LaSr)MnO_3$	53.0 ± 0.6	78.2

shown in Figs 5 to 8 where the effects of increases in decomposition temperature can be seen. In general, it is evident that the amorphous fluffy appearances of the precursors change to become more broken-up and particulate as the decomposition temperature is increased. Eventually well-separated oxide crystals are obtained at decomposition temperatures of the order of 1100° C. However, at temperatures above 1000° C the particles increase in size and generally become more sintered together.

The measurements of surface area of $LaMnO_3$ and $SrMnO_3$ produced at 1000° C and the $La_{1-x}Sr_xMnO_3$ produced at various temperatures are presented in Table V. It is clear that these measurements conducted on larger sized samples than those used in the scanning electron microscope reinforce the morphological observations made using the electron-optical technique and hence indicate that truly representative samples were used to obtain the micrographs shown in Figs 5 to 8. The data presented in Table V are the averages of at least three measurements made for each sample. Table VI shows the particle sizes of the various oxide samples calculated from the surface area measurements assuming a spherical

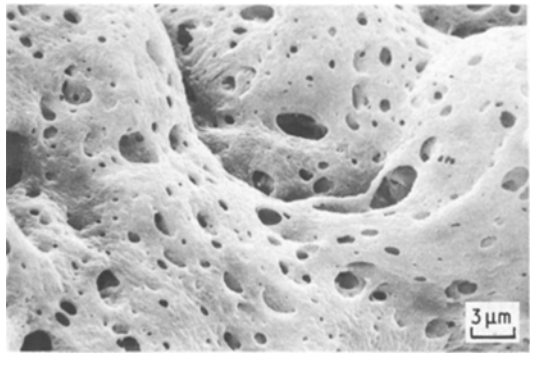

Figure 5 Scanning electron micrograph of Mn_2O_3 produced at 500° C.

TABLE III Phases identified by X-ray diffraction analysis

Precursor of:	Decomposition/oxidation temperature (° C)									
	Room temp.	200	300	400	500	600	800	900	1000	1100
Mn_2O_3	Amorphous (Am)	Am	Mn_3O_4	–	Mn_2O_3	Mn_2O_3	–	Mn_2O_3	Mn_3O_4	Mn_3O_4
$LaMnO_3$	Am	Am	MnO_2 (trace)	–	–	$LaMnO_3$	$LaMnO_3$	$LaMnO_3$	$LaMnO_3$	$LaMnO_3$
$SrMnO_3$	$Sr(NO_3)_2$	$Sr(NO_3)_2$	–	$Sr(NO_3)_2$	–	$SrCO_3$ $SrMnO_3$	$SrCO_3$ $SrMnO_3$	–	$SrMnO_3$	$SrMnO_3$
$(LaSr)MnO_3$	$Sr(NO_3)_2$ $SrCO_3$ (trace)	–	$Sr(NO_3)_2$ $SrCO_3$ (trace)	$SrCO_3$ $(LaSr)MnO_3$	– –	– –	$SrCO_3$ $(LaSr)MnO_3$	–	$(LaSr)MnO_3$	$(LaSr)MnO_3$

TABLE IV Carbon analysis of $La_{1-x}Sr_xMnO_3$

Temperature (° C)	Carbon content (wt%)	
	2 h	4 h
400	5.41	–
700	2.75	–
1000	0.80	0.41
1200	0.43	0.20
1400	0.09	0.07

geometry of the particles. These data again reinforce the electron-optical observations.

The results of the microanalysis of the strontium-substituted lanthanum manganite samples produced at 1100, 1200 and 1400° C are shown in histogram form in Figs 9 to 11. For each of the samples the integrated peak counts of the LaLα, SrKα and MnKα lines for each individual particle were obtained directly from the energy dispersive detector. The counts were subsequently converted to weight fractions using the technique developed by Cliff and Lorimer [15]. It was assumed that the particles were thin enough to allow X-ray absorption and fluorescence to be neglected.

4. Discussion

4.1. Production of Mn_2O_3

It is evident from the thermogravimetric and evolved gas analysis results presented in Fig. 1 that the major part of the weight loss associated with the decomposition/oxidation of the precursor of Mn_2O_3 is complete by 400° C. The small weight loss that can be seen to occur over the temperature range 930 to 980° C may be attributed to the thermal decomposition of Mn_2O_3 to yield Mn_3O_4 (as indicated by the X-ray diffraction data given in Table III). Consequently, in order to produce Mn_2O_3 from the precursor a final decomposition temperature between 400° C and 900° C is necessary for the removal of the nitrate and citrate.

The evolved gas analysis traces for m/e values of 18(H_2O^+), 30(NO^+) and 44(CO_2^+ and N_2O^+) show that the initial weight loss occurs as a result of dehydration. However, at temperatures above approximately 200° C the precursor decomposes/oxidizes rapidly in what appears to be a single-stage process yielding a mixture of CO_2 and N_2O which produces the ions CO_2^+ and N_2O^+ at m/e 44. It is interesting to note that the NO^+ ions at m/e 30, which occur as a cracking fragment of N_2O, are detected at the beginning of decomposition/oxidation only. Consequently, it is apparent that the N_2O is evolved only at the beginning of decomposition such that there may be a transitory existence of a citrate salt which is rapidly decomposed in the later stages of the process.

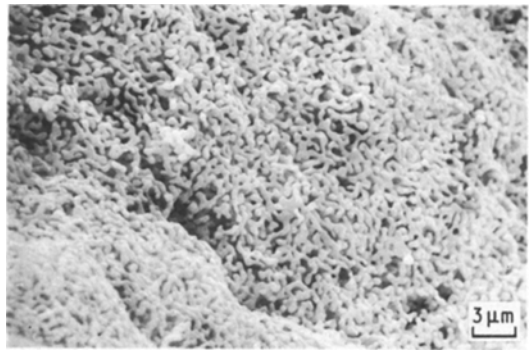

Figure 6 Scanning electron micrograph of Mn_3O_4 produced at 1000° C.

Previous work by Courty *et al.* [16] has recognized the existence of two types of pyrolysis reactions of citrate-nitrate precursors. Type I was characterized by a continuous and vigorous reaction and occurred with precursors containing Fe, Ni, Ag, Cu and Co which have a strong catalytic activity in oxidation processes. Such behaviour, also observed by Anderton and Sale [10] in the production of $LaCoO_3$ from citrate-nitrate gels, has apparently occurred in the present study of the production of Mn_2O_3. The second pyrolysis behaviour, Type II, is typified by a two-stage process in which an intermediate decomposition step occurs because of the formation of a stable semi-decomposed precursor consisting of a mixed citrate salt. Consideration of the evolved gas analysis data given in Fig. 1 indicates that this

TABLE V Surface-area measurements

Product/ time (h)	Surface area ($m^2 g^{-1}$)				
	Room temp.	700° C	1000° C	1200° C	1400° C
$LaMnO_3$/2			2.33 ± 0.05		
$SrMnO_3$/2			1.14 ± 0.09		
$La_{1-x}Sr_xMnO_3$/2	11.08 ± 0.20	18.77 ± 1.00	6.33 ± 0.20	2.57 ± 0.10	0.98 ± 0.04
/4		18.81 ± 1.01	6.26 ± 0.21	1.89 ± 0.12	0.10 ± 0.03

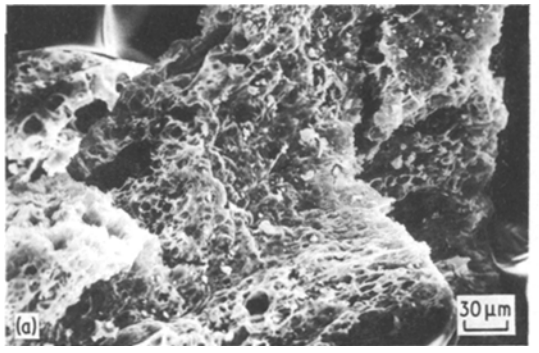

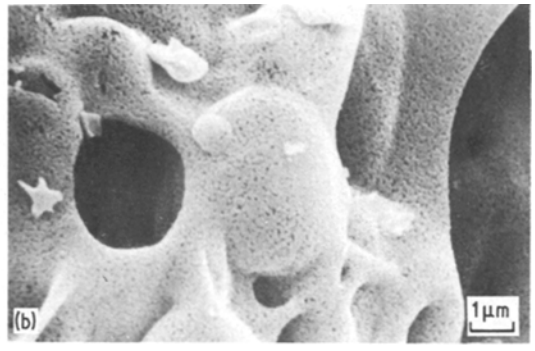

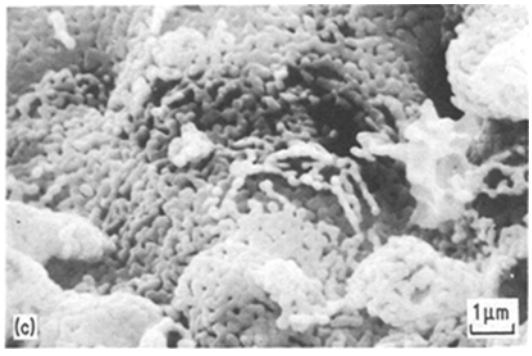

Figure 7 Scanning electron micrograph of $LaMnO_3$ produced at: (a) 600° C; (b) 900° C; (c) 1100° C.

general Type II behaviour may apply even in the single-step decomposition process (Type I). Consequently, it is apparent that the difference between Type I and Type II processes is not in the reaction mechanism; it is simply associated with the stability of the citrate produced on loss of the nitrate content from the precursor.

The actual weight loss determined for the production of Mn_2O_3 from the gel precursor was approximately 56% of the original sample weight. Calculations of the theoretical weight loss based on the stoichiometries of the metal nitrate and citric acid used in the original solutions yield a value of the order of 83% or a value of 79% if it is assumed that the water of crystallization of the original nitrate and citric acid is removed during the preparation of the precursor. This large difference between calculated and experimental weight losses indicates that the total amount of the nitrate and citric acid in the original solution is not maintained in the precursor.

Little evidence is available in the literature concerning the possible structural arrangements within amorphous gels. However, it is apparent from the evolved gas analysis that the precursor of Mn_2O_3 contains both citrate and nitrate ions, i.e. neither a metal nitrate (theoretical weight loss 68%) nor a metal citrate (theoretical weight loss 68.5%) are formed during precursor preparation. One structural arrangement that involves equimolar amounts of citric acid and manganese nitrate (as used in the original solution) may be represented as:

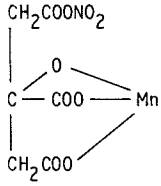

(1)

in which the manganese is triply charged (as in the final product) and the nitrate may be viewed as

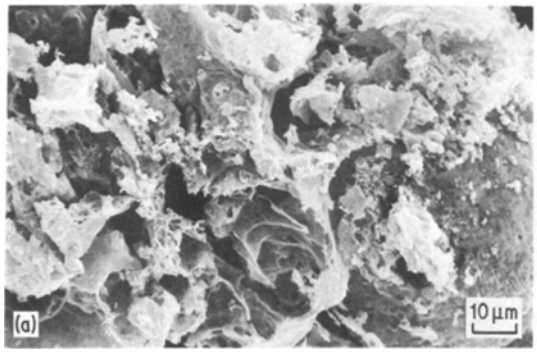

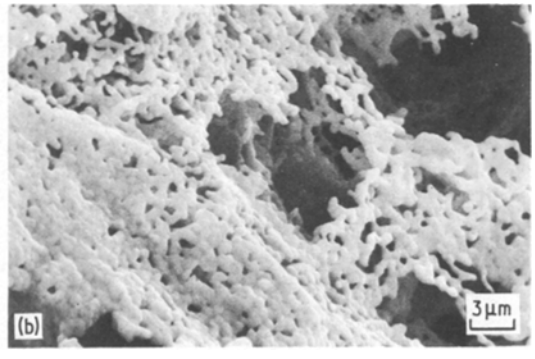

Figure 8 Scanning electron micrograph of $Sr_{0.5}La_{0.5}MnO_3$ produced at: (a) 800° C; (b) 1200° C.

TABLE VI Particle sizes calculated from surface areas

Product	Size after 2 h firing (μm)			
	Room temp.	700	1000	1200
$La_{1-x}Sr_xMnO_3$	0.20	0.03	0.07	0.29
$SrMnO_3$			1.79	
$LaMnO_3$			0.44	

either an NO_2 radical replacing one hydrogen from a COOH group, or as the NO_3 radical replacing the entire hydroxyl group from the COOH. Alternatively, other ways in which the metal nitrate may be complexed with citric acid may be presented as follows [17]:

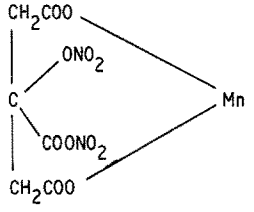

(2)

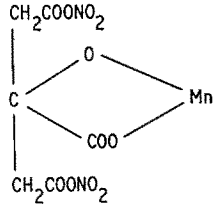

(3)

or

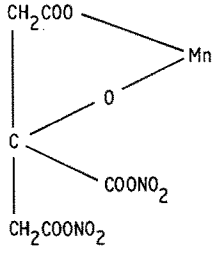

(4)

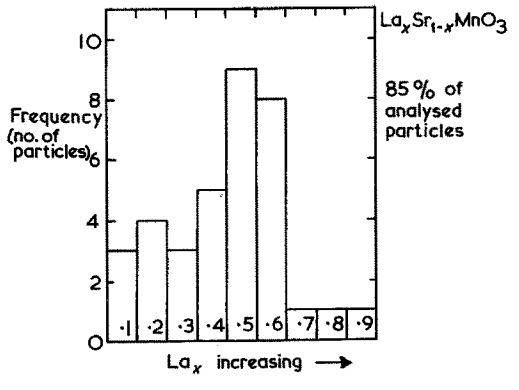

Figure 9 Homogeneity of $Sr_{1-x}La_xMnO_3$ produced at 1100° C.

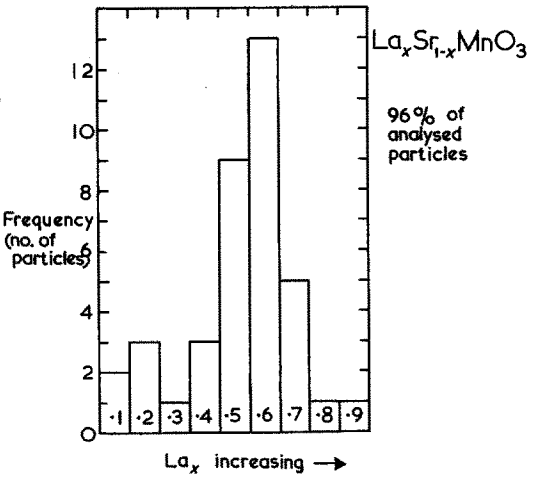

Figure 10 Homogeneity of $Sr_{1-x}La_xMnO_3$ produced at 1200° C.

In these three examples the manganese is divalent and the Mn^{2+} and NO_2 radicals replace either the hydrogen from COOH groups or from the OH group. The weight losses that may be predicted for the production of Mn_2O_3 from these possible structures (1–4) are 72.7, 76.4, 76.4 and 76.4 wt%, respectively, which are much larger than the experimentally determined value. Therefore, in order to explain the observed weight losses possible structural arrangements, in which the equimolar stoichiometric ratio of manganese nitrate to citric acid is not maintained, must be considered. Obviously many examples may be postulated, however, one complex based on the previous examples that seems to satisfy most requirements may be represented by:

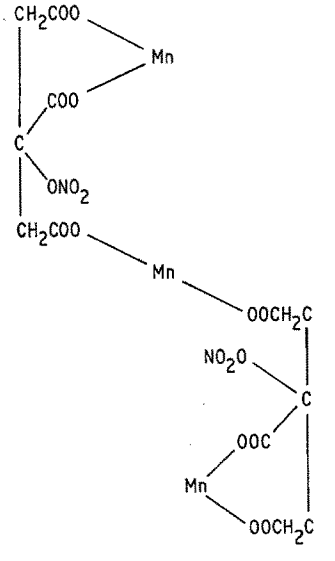

(5)

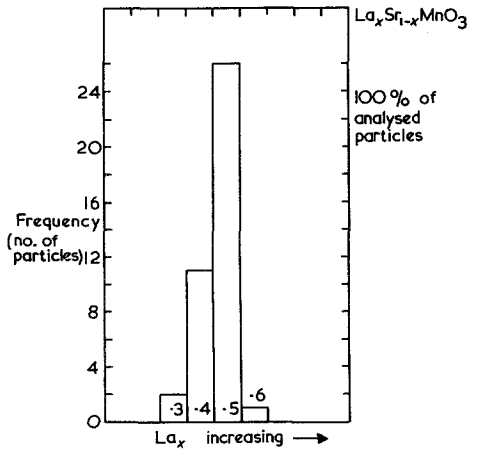

Figure 11 Homogeneity of $Sr_{1-x}La_xMnO_3$ produced at 1400° C.

The predicted weight loss for the production of Mn_2O_3 from such a complex is 62.5% which is in reasonable agreement with the experimental value. The formation of such a structure would allow some citric acid, water and nitrate ions to be lost during the preparation of the gel. For every three molecules of citric acid originally present one remains uncombined and may be removed from the mixture by either evaporation or decomposition to yield acetone, carbon dioxide and water during the precursor preparation in the vacuum oven. The formation of the proposed complex would also liberate three NO_3^- groups for each two molecules of $Mn(NO_3)_2$ originally present in solution. Consequently these ions would be available to produce nitric acid and various nitrogen oxides many of which were detected during precursor preparation. It must be emphasized that the proposed complex is only one possibility for the metal nitrate-citrate complex. Hence weight losses may only be used as approximate guides to the form of the complex, as a number of different complexing arrangements may occur in any one batch of precursor. A more detailed investigation of the organo-metallic chemistry of such complexes is beyond the scope of the present study.

The particle morphologies of the products obtained from the precursor were seen to change from the general fluffy amorphous appearance of the precursor to a more crystalline particulate solid as the decomposition/oxidation temperature was increased. The product obtained at 500° C (Fig. 5) can be seen to retain the amorphous appearance; however, well-defined pores are present in the solid and close examination reveals the early stages of formation of a particulate solid. Fig. 6 shows the Mn_3O_4 obtained from the precursor at 1000° C where it is evident that a "stringer-like" particle morphology has been obtained. This morphology represents an extension of the separation of the particulate solid from the amorphous mass as decomposition temperature is increased. Mn_2O_3 obtained at 900° C has the same appearance, although the size of the stringers is significantly smaller (0.1–0.2 μm thickness) as opposed to the 0.5–1 μm seen in Fig. 6. At temperatures above 1000° C the particulate size increased as sintering and thickening of the stringer-like morphology occurred.

4.2. Production of $LaMnO_3$

The thermogravimetric and evolved gas analysis data obtained for the decomposition/oxidation of the precursors of $LaMnO_3$ (Fig. 2) demonstrate that, in contrast to the precursor of Mn_2O_3, the decomposition process occurs in two well-separated stages over a wide range of temperature. The minimum temperature at which $LaMnO_3$ was detected by X-ray diffraction analysis was 600° C (see Table III). However, it can be seen from the thermogravimetric data that the product at this temperature has not achieved a constant weight, presumably because of some residual carbon, and so heating to a minimum temperature of 650° C is necessary in order to achieve $LaMnO_3$ of reasonable purity.

As NO^+ ions at m/e 30 were detected only in the first stage of the decomposition process it appears that a Type II pattern of decomposition, as indicated by Courty *et al.* [16], occurs for the precursor of $LaMnO_3$ such that a semi-decomposed citrate is obtained as the intermediary product between the two stages of decomposition. Such a two-stage process has also been identified in the production of $LaCrO_3$ from a citrate-nitrate precursor [10].

The experimental percentage weight loss obtained in the production of $LaMnO_3$ was approximately 50%. The theoretical weight loss based on the stoichiometry of the original solution is 78%, hence, as in the case of Mn_2O_3 it is obvious that some of the original citric acid and nitrate ions are not included in the precursor. On the basis of the possible complex postulated for the structural arrangement of the manganese citrate-nitrate precursor, a similar complex which would give a weight loss that agrees more closely

with the experimental data may be represented as:

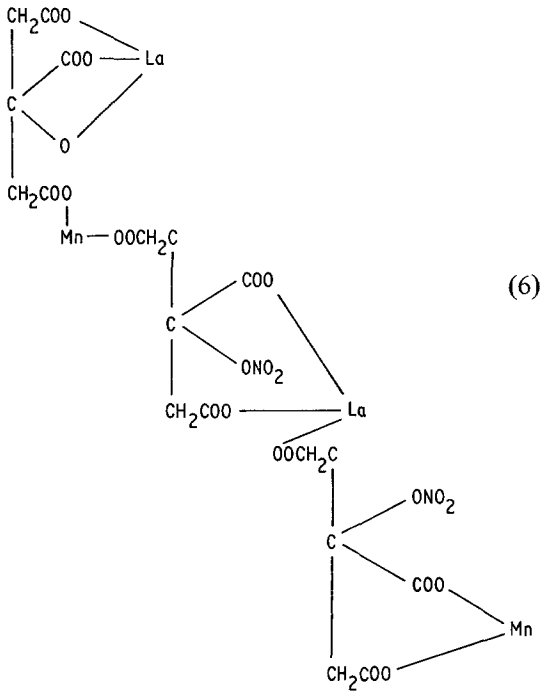

(6)

The theoretical weight loss based on the decomposition of this complex to yield $LaMnO_3$ is approximately 53%. In the complex the lanthanum is triply charged and replaces in one case the hydrogen of three –COOH groups (as in normal citrate formation) and in another case it replaces the hydrogen of one –OH group and two –COOH groups. Manganese in the divalent state replaces the hydrogen in two –COOH groups whilst NO_2 replaces the hydrogen of one –OH group.

The particle morphologies of the $LaMnO_3$ products obtained at 600, 900 and 1100° C are shown in Fig. 7 where it is evident that the dependence of morphology with temperature seen for Mn_2O_3 also occurs. However, $LaMnO_3$ retains an amorphous appearance up to higher temperatures than Mn_2O_3 and the $LaMnO_3$ particulate products are all smaller in particle size and less sintered together at a given temperature than the equivalent Mn_2O_3 samples. These observations imply that the diffusional processes required to produce the morphological changes are slower in $LaMnO_3$ than in Mn_2O_3 at any given temperature.

4.3. Production of $SrMnO_3$

The thermogravimetric and evolved gas analysis data obtained for the thermal decomposition/oxidation of the precursor of $SrMnO_3$ are presented in Fig. 3. It is evident that the decomposition process is complicated and quite unlike either of the reactions discussed for the decomposition of the precursors of Mn_2O_3 and $LaMnO_3$. The complete decomposition process to yield a constant weight product occurs in three separate stages over the temperature ranges 180–450° C, 550–650° C and 950–1030° C. X-ray diffraction analysis (Table III) showed that the precursor contained strontium nitrate. Consequently, one extra stage of decomposition associated with the thermal breakdown of this nitrate may be expected. However, X-ray diffraction analysis of the products of partial decomposition indicated that strontium carbonate was present in material obtained at temperatures between 600 and 1000° C. Strontium carbonate has been detected previously in the decomposition of precursors of strontium chromite and strontium cobaltite [10] and in the thermal decomposition of strontium formate [18]. In the present study strontium carbonate was detected at the same time as $SrMnO_3$, namely in the product of decomposition at 600° C. At this temperature strontium nitrate had disappeared from the product. Hence, it seems that strontium oxide produced from the nitrate reacted with carbon dioxide produced by combustion of the citrate to yield the carbonate. Consequently, in order to obtain $SrMnO_3$ that is not contaminated with strontium carbonate, decomposition temperatures in excess of 1000° C are required.

The evolved gas analysis data indicate that the first stage of decomposition consists of the breakdown of the citrate-nitrate in what appears to be a Type I pyrolysis reaction [16], although it is again evident, as in the case of the Mn_2O_3 precursor, that the nitrate is liberated first. The decomposition stage at 550–650° C is associated with the production of strontium oxide from the nitrate whilst the final stage at 950–1030° C is the decomposition of the strontium carbonate which is produced during the decomposition of the citrate-nitrate complex. An interesting observation from the evolved gas analysis data for the final stage of decomposition is the large size of the peak for m/e 28 (CO^+ or N_2^+) relative to the peak for m/e 44 (CO_2^+ or N_2O^+). Because a peak at m/e 30 (NO^+) is not present for this stage of the process and because oxygen (not air) was bled into the reactor it is apparent that the peak at m/e 28 is associated with CO^+ whilst that at m/e 44 is caused by CO_2^+. If the decomposition of strontium carbonate was a

normal carbonate decomposition of the type:

$$MCO_3(c) \rightarrow MO(c) + CO_2(g)$$

then the major peak would be CO_2^+ with CO^+ being present at a relative abundance of 11.4% in accordance with the mass spectra cracking pattern. However, from Fig. 3 it is evident that the peak at m/e 28 is of the order of ten times larger than the peak at m/e 44. The most probable explanation of this observation is that the CO_2 produced by decomposition reacted with free carbon present as a result of the incomplete oxidation of the citrate such that a simple two stage reaction occurred:

$$SrCO_3(c) \rightarrow SrO(c) + CO_2(g)$$

$$CO_2(g) + C(gr) \rightarrow 2CO(g)$$

to give $SrCO_3(c) + C(gr) \rightarrow SrO(c) + 2CO(g)$

As for the precursors of Mn_2O_3 and $LaMnO_3$, the weight loss determined experimentally shows that not all the citric acid and nitrate ions present in the original solution are combined in the precursor. It is anticipated that a complex similar to the one postulated for the precursor of $LaMnO_3$ is produced with the substitution of some strontium for lanthanum or manganese, even though it is obvious from the X-ray diffraction data that a detectable proportion of strontium precipitated as strontium nitrate and was not included in the complex.

The particle morphologies of the product $SrMnO_3$ were almost identical to those observed for $LaMnO_3$. The fluffy amorphous product was observed at temperatures up to 800° C. Particulate products, with particle size of 2.0 μm at 1050° C and 3.5 μm at 1200° C were obtained at higher decompositon temperatures. The $SrMnO_3$ particles were slightly larger than equivalent $LaMnO_3$ particles at any given temperature. The additional particle growth may have occurred as a result of the high temperature decomposition of strontium carbonate to yield oxide which is eventually incorporated in the perovskite.

4.4. Production of $Sr_{0.5}La_{0.5}MnO_3$

4.4.1. Precursor decomposition/oxidation

From the thermogravimetric and evolved gas analysis data given in Fig. 4 it is apparent that, as for the production of $SrMnO_3$, decomposition temperatures in excess of 1000° C are required to yield a product of constant weight. X-ray diffraction analysis of the precursor and semi-decomposed products again revealed the existence of strontium nitrate and carbonate although both were at much lower concentrations than in the production of $SrMnO_3$. The complete decomposition, therefore, may be explained in the manner used for $SrMnO_3$. The major decomposition of the precursor occurs in a single-stage Type I process over the temperature range 180– 450° C. Evolved gas analysis again reveals that the nitrate ions are released from the complex prior to the combustion of the citrate. The following two stages of decomposition, with much smaller associated weight losses, involve the decomposition of strontium nitrate and carbonate, respectively, as temperature increases.

4.4.2. Particle morphology and composition

The particle morphologies of the strontium-substituted $LaMnO_3$ were very similar to those seen for the products $LaMnO_3$ and $SrMnO_3$. At low decomposition temperatures (below 800° C) the products retain a fluffy amorphous appearance (see Fig. 8). A particulate product is obtained at temperatures in excess of 800° C with the particle size increasing with increasing temperature. At 1200° C (Fig. 8) the particles become regular and well-rounded and are approximately 0.5–1 μm in size. Sintering of the particles was evident in the product obtained at 1300° C. Although some of the strontium had separated from the precursor in the form of nitrate and carbonate no evidence of gross separation was visible in any material examined in the scanning electron microscope.

Compositional homogeneity is of major importance in the potential use of the strontium-substituted $LaMnO_3$. The microanalysis of particles produced at 1100, 1200 and 1400° C are presented in Figs 9 to 11, respectively, in which the frequency of particles having stoichiometries ranging from $La_{0.1}Sr_{0.9}MnO_3$ to $La_{0.9}Sr_{0.1}MnO_3$ are plotted as histograms. Single-oxide and double-oxide particles were discounted. Most rejected particles were, in fact, double oxides, i.e. either $LaMnO_3$ or $SrMnO_3$. It can be seen from the histograms that as the precursor decomposition temperature is increased the percentage of particles falling within the compositional range of interest increases, e.g. 85% at 1100° C, 96% at 1200° C and 100% at 1400° C. In addition, the band of inhomogeneity, i.e. departure from $La_{0.5}Sr_{0.5}MnO_3$, decreased. At 1100° C approximately 37% of the particles were

in the compositional range $La_{0.4}Sr_{0.6}MnO_3$ to $La_{0.6}Sr_{0.4}MnO_3$. At 1200° C, 50% of the particles were within this compositional band, whilst at 1400° C, 64% of the particles were $La_{0.5}Sr_{0.5}MnO_3$ and the remainder had compositions in the range $La_{0.3}Sr_{0.7}MnO_3$ to $La_{0.6}Sr_{0.4}MnO_3$. The wide range of homogeneity at lower temperatures was a result of the segregation of $Sr(NO_3)_2$ during precursor preparation and the production of $SrCO_3$ during precursor decomposition. Nevertheless, the yields of particles are very impressive when compared with the results of the production of similar perovskites by the freeze-drying technique (60%) and by the conventional heating, milling and re-heating of mixtures of oxides and carbonates (60%) [10] and so indicate the potential of the process for the production of uniformly substituted perovskite oxides.

4.4.3. Carbon content and surface area

The major problem with the amorphous gel processes in which poly-functional organic acids are used as gelling agents in the residual carbon present after precursor decomposition/oxidation. Table IV shows the weight percentage of carbon detected in the substituted perovskite after firing in air at various temperatures for periods of 2 and 4 h. From the thermogravimetric data it is apparent that temperatures in excess of 1000° C are required to remove $SrCO_3$ from the product. Consequently, it is not surprising to find that the low-temperature products contained appreciable carbon either in the form of carbonate or free carbon left as the result of citrate decomposition. However, the levels of carbon found after firing for 2 h at 1200° C and 1400° C, 0.43 and 0.09 wt%, respectively, are also high and may have effects upon either the sintering characteristics or the catalytic properties of the powders. Firing at 1000, 1200 and 1400° C for 4 h reduced the carbon levels to 0.41, 0.20 and 0.07 wt%, respectively, and so indicated the advantage of extended firing periods. It is anticipated that these levels could be lowered significantly by carrying out the precursor decomposition/oxidation in oxygen.

The sinterability of the substituted perovskite and its use in catalytic applications may also be governed by the overall surface area/particle size of the powder. Tables V and VI show the surface area and particle size calculated from the surface area, based on the assumption of a spherical particle morphology, for various oxide samples produced in this study. It is evident that decomposition of the precursor of the substituted perovskite at 700° C causes an increase in the surface area of the product. However, as the decomposition/oxidation temperature is increased the surface area of the powder is reduced accordingly. From powder processing considerations the product obtained at 1200° C after 2 h firing is still a fine powder (approximately 0.3 μm particle size); however, a significant reduction in surface area has occurred (from 18.77 $m^2 g^{-1}$ at 700° C to 2.57 $m^2 g^{-1}$ at 1200° C). Consequently, there is a conflict between the experimental conditions required for high surface area and low carbon content. Extended periods at elevated temperatures minimize the residual carbon while short periods at low temperatures maximize the surface area. Undoubtedly, the best compromise would appear to be an initial treatment of the precursor at 700° C to yield the high surface area followed by an increase in temperature to 1100° C for a period of up to 4 h to remove carbon. Temperatures in excess of 1100° C for this second stage should be avoided as these would inevitably lead to a decrease in surface area as indicated by the data given in Table V.

5. Conclusions

(1) The amorphous citrate process has been used to produce strontium-substituted lanthanum manganite with a process yield of 85% at 1100° C, 96% at 1200° C and 100% at 1400° C. These figures compare well with the yields of freeze-drying and conventional thermal decomposition/sintering/grinding processes.

(2) The range of inhomogeneity of substitution of strontium for lanthanum was found to decrease with increasing firing temperature.

(3) Conflicting experimental requirements exist for the production of high surface area and low residual carbon content material. High surface areas are obtained with short decomposition times at low temperature; however, low residual carbon contents are obtained with long decomposition periods at elevated temperatures.

(4) The process has also been used to produce Mn_2O_3, Mn_3O_4, $LaMnO_3$ and $SrMnO_3$ powders.

Acknowledgements

The authors would like to express thanks to Professors E. Smith and K. M. Entwistle for the provision of laboratory facilities in the joint Uni-

versity of Manchester/UMIST Metallurgy Building.

References

1. D. W. JOHNSON and F. J. SCHNETTLER, *J. Amer. Ceram. Soc.* **53** (1970) 440.
2. A. LANDSBERG and T. T. CAMPBELL, *J. Met.* **17** (1965) 856.
3. F. K. ROEHRIG and T. R. WRIGHT, *J. Vac. Sci. Technol.* **9** (1972) 1368.
4. F. R. SALE, *Metall. Mater. Technol.* **9** (1977) 439.
5. J. M. FLETCHER and C. J. HARDY, *Chem. Ind.* **87** (1968) 48.
6. C. MARCILLY, P. COURTY and B. DELMON, *J. Amer. Ceram. Soc.* **53** (1970) 56.
7. B. DELMON and J. DROGUEST, in "Fine Particles – Second International Conference", edited by W. E. Kuhn and J. Ehretsmann (The Electrochemical Society, New Jersey, 1974) p. 242.
8 D. J. ANDERTON and F. R. SALE, *Powder Metall.* **22** (1979) 8.
9. A. C. C. TSEUNG and H. L. BEVAN, *J. Mater. Sci.* **5** (1970) 604.
10. D. J. ANDERTON and F. R. SALE, *Powder Metall.* **22** (1979) 14.
11. D. MEADOWCROFT, Proceedings of the International Conference on Strontium-containing Compounds, edited by T. J. Gray (Atlantic Ind. Research Institute, Halifax, Nova Scotia, 1973) p. 120.
12. R. J. H. VOORHOEVE, J. P. REMEIKA, P. E. FREELAND and B. T. MATTHIAS, *Science* **177** (1972) 353.
13. G. PARRAVANO, *J. Amer. Chem. Soc.* **15** (1953) 1497.
14. G. SANDSTEDE and E. ROBINS, *Chem. Ing. Tech.* **32** (1960) 413.
15. G. W. LORIMER and G. CLIFF, *J. Microscopy* **103** (1975) 203.
16. P. COURTY, H. AJOT, C. MARCILLY and B. DELMON, *Powder Technol.* **7** (1973) 21.
17. S. KIRSCHNER and R. KIESLING, *J. Amer. Chem. Soc.* **82** (1960) 4174.
18. D. DOLLIMORE, J. P. GUPTA and D. V. NOWELL, in "Proceedings of the First European Symposium on Thermal Analysis" (The Chemical Society, London, 1976) p. 233.

Received 18 January
and accepted 22 February 1982